REPORT DOCUMENTATION PAGE

1 AGENCY USE ONLY	2 REPORT DATE JULY 93	3 TYPE/DATES COVERED
4 TITLE AND SUBTITLE MODELLING SHOCK INITIATION AND DETONATION IN THE NON-IDEAL EXPLOSIVE PBXW-115		5 FUNDING NUMBERS
6 AUTHOR DAVID L KENNEDY AND DAVID A JONES		
7 FORMING ORG NAMES/ADDRESSES DEFENCE SCIENCE AND TECHNOLOGY ORGANIZATION, MATERIALS RESEARCH LABORATORY, PO BOX 50, ASCOT VALE VICTORIA 3032 AUSTRALIA		8 PERFORMING ORG. REPORT NO
09 SPONSORING/MONITORING AGENCY NAMES AND ADDRESSES		
11 SUPPLEMENTARY NOTES		
12 DISTRIBUTION/AVAILABILITY STATEMENT DISTRIBUTION STATEMENT A		12B DISTRIBUTION CODE

13. ABSTRACT (MAX 200 WORDS): WE ANALYSE THE DETONICS OF THE NON-IDEAL EXPLOSIVE PBXW-115 (ALSO CALLED PBXN-111). TWO CHEMICAL EQUILIBRIUM CODES WERE USED TO PREDICT ITS IDEAL CJ STATE, WITH ESTIMATES OF ITS IDEAL DETONATION VELOCITY DIFFERING BY OVER 1 3MM US1. A SMALL DIVERGENT DETONATION THEORY WAS CALIBRATED TO UNCONFINED DETONATION VELOCITY MEASUREMENTS, AND USED TO DESCRIBE THE CJ STATE AT DIFFERENCT CHARGE DIAMETERS. IT WAS PREDICTED THAT THE DETONATION WAS BEING SUPPORTED BY ABOUT 15% REACTION AT THE CRITICAL DIAMETER, WITH THE VELOCITY ABOUT 1.7MMUS1 BELOW THE IDEAL VALUE. A FINITE ELEMENT HYDROCODE WAS USED TO SIMUALTE A VARIETY OF INITIATION AND DETONATION TESTS, WITH THE RESULTS GENERALLY IN EXCELLENT AGREEMENT WITH THE EXPERIMENTAL DATA. IT WAS FOUND THAT MANY EXPERIMENTAL TECHNIQUES (INCLUDING THOSE FOR THE MEASUREMENT OF IDEAL DETONATION VELOCITY, CJ ZONE LENGTH, AND POP-PLOTS) REQUIRE SUBSTANTIALLY DIFFERENT INTERPRETATION FOR NON-IDEAL EXPLOSIVES.

14 SUBJECT TERMS			15 NUMBER OF PAGES 9 16 PRICE CODE
17 SECURITY CLASS.REPORT UNCLASSIFIED	18 SEC CLASS PAGE UNCLASSIFIED	19 SEC CLASS ABST.	20 LIMITATION OF ABSTRACT UNCLASSIFIED

MODELLING SHOCK INITIATION AND DETONATION IN THE NON-IDEAL EXPLOSIVE PBXW-115

David L. Kennedy
Mining Services Technology Centre,
ICI Australia Operations Pty. Ltd.
PO Box 196, George Booth Drive,
Kurri Kurri NSW 2327, Australia

David A. Jones
DSTO Materials Research Laboratory
PO Box 50, Ascot Vale 3032, Australia

Paper to be presented at the 10th International Symposium on Detonation,
to be held July 12 to July 16, 1993, Boston, USA

MODELLING SHOCK INITIATION AND DETONATION IN THE NON-IDEAL EXPLOSIVE PBXW-115

David L. Kennedy
ICI Australia Operations Pty. Ltd.
PO Box 196, Kurri Kurri NSW 2327, Australia

David A. Jones
DSTO Materials Research Laboratory
PO Box 50, Ascot Vale 3032, Australia

We analyse the detonics of the non-ideal explosive PBXW-115 (also called PBXN-111). Two chemical equilibrium codes were used to predict its ideal CJ state, with estimates of its ideal detonation velocity differing by over 1.3 mm.μs^{-1}. A small divergent detonation theory was calibrated to unconfined detonation velocity measurements, and used to describe the CJ state at different charge diameters. It was predicted that the detonation was being supported by about 15% reaction at the critical diameter, with the velocity about 1.7 mm.μs^{-1} below the ideal value. A finite element hydrocode was used to simulate a variety of initiation and detonation tests, with the results generally in excellent agreement with the experimental data. It was found that many experimental techniques (including those for the measurement of ideal detonation velocity, CJ zone length, and Pop-plots) require substantially different interpretation for non-ideal explosives.

INTRODUCTION

Composite explosives are used extensively in both commercial and military applications. The partial or complete physical separation of their oxidiser and fuel phases results in mass diffusion reducing their reaction rates and increasing their reaction zone lengths in comparison with monomolecular explosives. As a consequence, they exhibit non-ideal performance, where their detonation velocities can be considerably lower than the ideal value predicted by equilibrium thermodynamic calculations. They typically have large critical diameters. These factors all contribute to increased difficulty and expense when performing characterisation experiments, as the charge weights involved are necessarily larger than those involving ideal explosives. This raises the question as to how relevant existing experimental techniques are for the investigation of the detonics of such explosives.

This paper will present a detailed evaluation of the experimental techniques applied to the non-ideal explosive PBXW-115 (also known as PBXN-111). These include detonation velocity and critical diameter for both unconfined and confined charges, corner turning ability, and shock front curvature, all obtained at NSWC by Forbes and coworkers[1,2] for the US variant. Bocksteiner et al.[3] at MRL have measured detonation velocity and critical diameter for both unconfined and confined charges of the Australian variant, examining the effects of RDX and Al particle size. Held[4] has applied a small-sample technique to the measurement of the ideal detonation velocity of the German variant.

The results will include a description of the ideal Chapman-Jouget (CJ) detonation state as provided by two equilibrium thermodynamic codes, an analysis of steady detonation in axisymmetric geometry, and time-resolved numerical simulations using the hydrocode DYNA2D.[5]

IDEAL DETONATION — THE IDEAL CJ STATE

The nominal density of PBXW-115 is about 1.79 g.cm^{-3}, corresponding to voidage levels of less than 2%. It is cast cured, with its nominal composition being 20% cyclotrimethylene trinitrate (RDX), 43% ammonium perchlorate (AP), 25% aluminium (Al), and 12% hydroxy terminated polybutadiene (HTPB) as binder.

Two chemical equilibrium codes were used to calculate its CJ state for an ideal detonation, with the results presented in Table 1. The first was BKW,[6] based on the Becker-Kistiakowsky-Wilson equation of state (EoS) for the gaseous products and the Cowan EoS for the solid products. The second was the ICI code IDeX (standing for Ideal Detonation of eXplosives), using an intermolecular EoS[7] for the gaseous products and the Murnaghan EoS for the solid products.

TABLE 1. IDEAL CJ STATE OF PBXW-115

Parameter	BKW	IDeX
Detonation velocity (mm.μs^{-1})	8.010	6.665
Detonation pressure (GPa)	27.51	22.53
Detonation temperature (K)	5175	5295
Heat of reaction (MJ.kg^{-1})	6.328	8.396
CJ Gamma	3.175	2.534

The predictions from the two codes differ to a greater extent than has been observed for any other explosive. Some of this would be due to the treatment of the binder — the BKW calculation used an existing plasticiser ($C_{41}H_{76}O_6$) from its database, while the IDeX calculation used a closer estimate of the composition ($C_{70}H_{110}O_1$). Several IDeX calculations were performed with this binder replaced by typical plasticisers — in all cases, the results were similar, with nothing approaching the BKW results.

Table 2 summarises the predicted equilibrium detonation products. There are slight differences due to the codes allowing different product species. However, the major effect is believed to be due to the differences in the compressibilities between the Cowan and the Murnaghan EoS descriptions of graphite. This would affect the C(graphite)/CO balance, causing a subsequent shift in the H_2/H_2O balance.

TABLE 2. PREDICTED DETONATION PRODUCTS

Species	Mole numbers (1 kg explosive)	
	BKW	IDeX
CH_4	n.a.#	0.407
CO	0.443	5.30
CO_2	0.0158	0.232
H_2	8.66	13.7
H	0.0510	n.a.#
NH_3	n.a.#	1.69×10^{-3}
H_2O	6.75	0.498
HCl	2.90	3.66
Cl_2	0.382	Nil
N_2	4.53	4.53
NO	4.09×10^{-3}	Nil
C (diamond)	n.a.#	Nil
C (graphite)	9.64	5.46
Al_2O_3	4.63	4.63

Not available in product species database.

The IDeX predictions have been adopted, for the pragmatic reason that the subsequent CPeX analysis (described below) based on the BKW predictions could not be made to fit the experimental detonation velocity data.

REACTIVE EQUATION OF STATE MODEL

The unreacted or explosive phase is described by a Mie-Grüneisen EoS in the form

$$e_x = e_r + \frac{v_{x0}}{\Gamma_{x0}}(p_x - p_r) \tag{1}$$

where p is pressure, v is specific volume, e is specific internal energy, and Γ is the Grüneisen coefficient. The subscripts are: x for the unreacted explosive, 0 for the initial state, and r for the reference (principal) isentrope. The latter is represented by the Birch-Murnaghan finite strain equation in the form described by Jeanloz[8] as

$$p_r = 3K_0\,\varphi(2\varphi+1)^{5/2}\left[1+a_1\varphi\right] \tag{2}$$

and

$$e_r = \frac{9}{2}K_0\,v_{r0}\,\varphi^2\left[1+(2a_1/3)\varphi\right] \tag{3}$$

where

$$\varphi = \frac{1}{2}\left[(v_{x0}/v_x)^{2/3}-1\right] \tag{4}$$

The required coefficients in equations (2) to (4) are determined from the Hugoniot

$$U = c_0 + s\,u \tag{5}$$

where U is shock velocity and u particle velocity, as

$$K_0 = \rho_{x0}\,c_0^2 \quad \text{and} \quad a_1 = (3/2)(4s-5) \tag{6}$$

The reacted or product phase, denoted by the subscript p, is described by a polytropic EoS with a density-dependent index, namely

$$e_p = \frac{p_p v_p}{\gamma_p - 1} - q_p \tag{7}$$

where

$$\gamma_p = \gamma_0 + \gamma_1/v_p + \gamma_2/v_p^2 \tag{8}$$

and where q_p is the heat of reaction. The constants in equation (8) are determined by requiring that it return the correct values for $(\partial \ln p/\partial \ln v)_s$ at the ideal CJ state and at infinite expansion.

The equation of state for the reacting mixture is then completely specified by invoking the simple mixture rules

$$p \equiv p_x \equiv p_p,\; v \equiv v_x \equiv v_p,\; e = (1-\lambda)e_x + \lambda\, e_p \tag{9}$$

where λ is the extent of reaction, varying from 0 for the unreacted explosive to 1 for the detonation products. The associated reaction rate was developed for composite porous explosives by Kirby and Leiper,[9] namely

$$\dot{\lambda} = (1-\lambda)\left\{\frac{p_{hs}a_h}{\tau_h} + \frac{p\,a_i}{\tau_i} + \frac{p\,a_f}{\tau_f}\right\} \tag{10}$$

where

$$p_{hs} = \begin{cases} \dfrac{p}{4}\left(\dfrac{3p}{4p_{cr}}\right)^3 & \text{for } p < 4p_{cr}/3 \\ p - p_{cr} & \text{for } p \ge 4p_{cr}/3 \end{cases} \tag{11}$$

The subscripts are: h for hotspot, i for intermediate, and f for final stages of the reaction. There are four adjustable parameters — three characteristic reaction times τ, and the critical pressure p_{cr} that inhibits the onset of the hotspot reaction. The a factors in equation (10) describe the assumed geometry of the burn front, controlling the switching on and off of the hotspot, intermediate and final reaction rate terms. They are functions of λ, and are Gaussian in shape, namely

$$a_h = \begin{cases} \exp\left\{-\left[(\lambda - C_i)/W_h\right]^2\right\} & \text{for } 0 \le \lambda \le C_i \\ \exp\left\{-\left[(\lambda - C_i)/W_i\right]^2\right\} & \text{for } C_i < \lambda \le 1 \end{cases} \tag{12}$$

$$a_i = \begin{cases} 0 & \text{for } 0 \le \lambda \le C_i \\ 1 - a_h & \text{for } C_i < \lambda \le C_f \\ \exp\left\{-\left[(\lambda - C_i)/W_h\right]^2\right\} - a_h & \text{for } C_f < \lambda \le 1 \end{cases} \tag{13}$$

$$a_f = \begin{cases} 0 & \text{for } 0 \le \lambda \le C_f \\ 1 - a_h - a_i & \text{for } C_f < \lambda \le 1 \end{cases} \tag{14}$$

where the Gaussian parameters are defined in terms of the mass fractions, Φ, of the three stages as:

Centroids

$$\begin{cases} C_i = \Phi_h^2 \\ C_f = (\Phi_h + \Phi_i)^2 \end{cases} \tag{15}$$

Half-widths

$$\begin{cases} W_h = 2C_i/(1+C_i) \\ W_i = \Phi_h(1-\Phi_h) \\ W_f = \Phi_f(1-\Phi_f) \end{cases} \tag{16}$$

STEADY NONIDEAL DETONATION - CPeX ANALYSIS

The above reactive equation of state was embedded into the analytical non-ideal detonation model CPeX (standing for Commercial Performance of eXplosives). This model was developed to describe the detonics of non-ideal explosives by Kirby and Leiper,[9] who extended the small divergent detonation theory of Wood and Kirkwood.[10] It describes the flow along the central streamtube between the detonation front and the CJ plane for unconfined cylindrical geometry by using the shooting method described by Braithwaite et al.[11] to solve the system of partial differential equations including the Euler equations of motion, the equation of state, the reaction rate, and an empirical relationship between the wave front curvature R_s and the charge diameter d. In previous versions of CPeX, this relationship had the form

$$R_s = (d - Bx_{CJ})/A \qquad (17)$$

where x_{CJ} is the CJ zone length at the diameter d, and where A and B are empirical constants. However, in practice, x_{CJ} is not known beforehand, so that an iterative procedure must be employed to determine the necessary model constants. This work employs a simpler form suggested by Leiper,[12] namely

$$\frac{d}{R_s} = \alpha + \beta \frac{d_{cr}}{d} \qquad (18)$$

where α and β are empirical constants and d_{cr} is the critical diameter below which detonation will not propagate.

The adjustable parameters in the reaction rate law were varied until the predicted variation of detonation velocity with unconfined charge diameter matched the experimental measurements of Forbes et al.[1] as shown in Figure 1. This figure also includes CPeX fits to an ideal and a non-ideal explosive for comparative purposes. The former is the fine RDX Composition B (COMP B) data of Malin.[13] The latter is a proprietary ICI blend of porous ammonium nitrate prill plus fuel oil (ANFO) with an AN/water-in-oil emulsion.

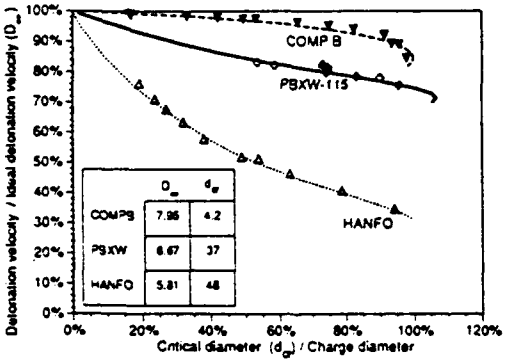

FIGURE 1. DETONATION VELOCITY FOR UNCONFINED CYLINDRICAL CHARGES

The ideal detonation velocity assumed in the CPeX fit for PBXW-115 is about 0.5 mm.μs^{-1} faster than that determined by a linear extrapolation of Forbes' data. It is believed that the experimental data have been obtained over too small a range of diameters, being limited to within a factor of two of the critical diameter. As an illustrative example, the "ideal" detonation velocity inferred for HANFO from measurements made on charges up to twice the critical diameter is about 1.5 mm.μs^{-1} lower than the value predicted from ideal thermodynamic calculations, and inferred from measurements over a wider range of charge diameters (namely up to six times the critical diameter).

The parameter values for PBXW-115 are summarised in Table 3, applying specifically to the NSWC composition.[1,2] For reasons not yet identified, the Australian variant[4] has a critical diameter roughly twice that of the NSWC material.

Since a Hugoniot has not been published for PBXW-115, one was derived from those of its components using the mixture rule described by Afanasenkov et al.[14] — this Hugoniot is similar to that measured experimentally for the propellant SPIS-44 with composition 20 / 49 / 21 / 10% HMX / AP / Al / binder, for which $U = 2.774 + 1.855u$.[15]

TABLE 3. CPeX MODEL CONSTANTS FOR PBXW-115

Parameter	Symbol	Value
Initial density	ρ_0	1.79 g.cm^{-3}
Hugoniot intercept	c_0	2.80 mm.μs^{-1}
Hugoniot slope	s	1.83
Grüneisen coefficient	Γ_{x0}	2.60
Curvature parameter	α	0.165
Curvature parameter	β	0.692
Polytropic coefficient	γ_0	1.343
Polytropic coefficient	γ_1	0.2045 cm^3 g^{-1}
Polytropic coefficient	γ_2	0.005112 cm^6 g^{-2}
Hotspot mass fraction	Φ_h	0.15
Intermediate mass fraction	Φ_i	0.60
Final mass fraction	Φ_f	0.25
Critical hotspot pressure	p_{cr}	5.5 GPa
Hotspot time constant	τ_h	11.8 μs. GPa^{-1}
Intermediate time constant	τ_i	100.0 μs. GPa^{-1}
Final time constant	τ_f	66.0 μs. GPa^{-1}

Initially, the CPeX fit for PBXW-115 was based on the plausible assumption that the hotspot or initial reaction consumed the RDX, that the intermediate phase of the reaction involved the AP plus binder, and that the Al was the last to react. The appropriate mass fractions would then be $\Phi_h = 20\%$, $\Phi_i = 55\%$ and $\Phi_f = 25\%$. However, a superior fit to the velocity data was achieved by modifying the hotspot mass fraction to be $\Phi_h = 15\%$ (with $\Phi_i = 60\%$.) This may indicate that the Gaussian shape factors developed for highly porous explosives and described in equations 12 to 16 are not as appropriate for non-porous explosives. Alternatively, it may be argued that the use of a single parameter, λ, is not sufficient to simultaneously account for the release of energy via the chemical reactions, the switch from unreacted to reacted equations of state, and the geometry of the burn front.

It should be noted that the adopted values of the constants describing the late stages of the reaction (ie. Φ_i, Φ_f, τ_i and τ_f) are not unique — other assumed values could give equally acceptable fits to the detonation velocity data. This is explained by examining the reaction rate in greater detail. Figure 2 shows how the predicted CJ extent of reaction varies with charge diameter. Detonation in the ideal explosive COMP B fails when its CJ extent of reaction falls below 96%, whereas both the non-ideal compositions continue to propagate down to about 15% reaction. The maximum CJ extent of reaction achieved over the range of diameters sampled for PBXW-115 is about 35%. Consequently, that part of the reaction rate for $\lambda > 0.35$ has not been fitted to

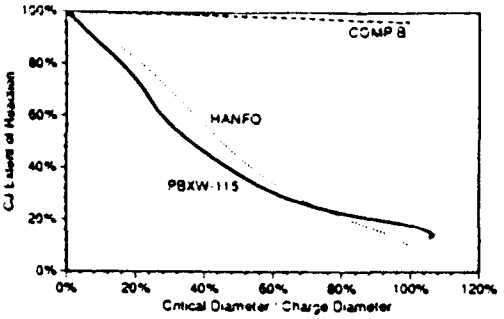

FIGURE 2. CPeX CJ EXTENT OF REACTION

experimental data, and so must be considered conjectural.

Figure 3 examines this in greater detail, by presenting the full reaction rate surface $\dot{\lambda}(p,\lambda)$ for each explosive. The (p_{CJ},λ_{CJ}) locus (traced out by varying charge diameter) for unconfined detonation is superimposed on this surface, together with the two (p,λ) histories followed by Lagrangian

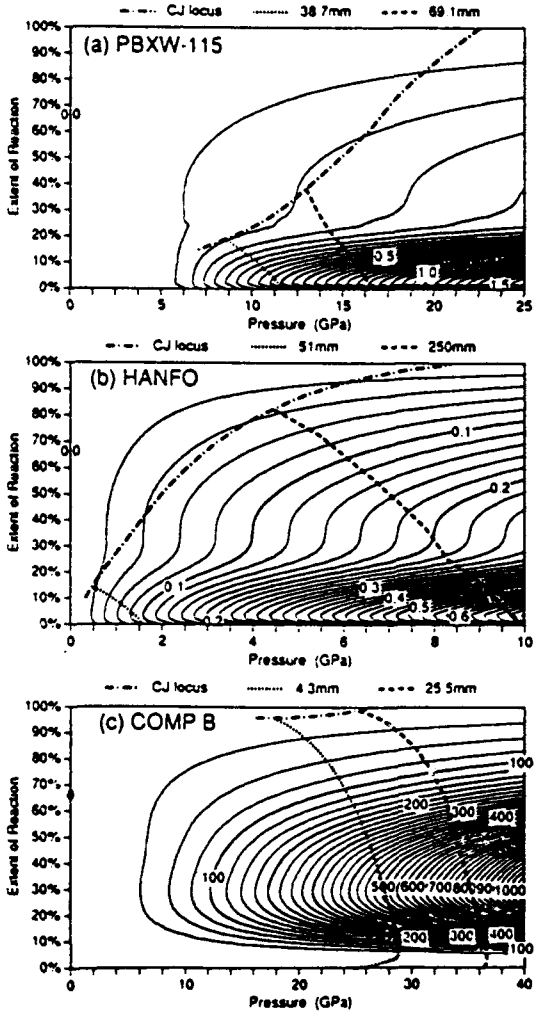

FIGURE 3. CONTOURS OF REACTION RATE $\dot{\lambda}(p,\lambda)$

particles on the central streamtube between the shock front and the CJ plane for unconfined detonations in the smallest and largest diameters characterised experimentally. It can be seen that the detonation velocity measurements performed to date have sampled only a very restricted subset of the reaction rate surface for PBXW-115, so that any predictions of late-time reactions involving the AP and Al must be of dubious accuracy. In order to extract accurate values for the time constants τ_i and τ_f from a CPeX analysis, it would be necessary to measure the detonation velocity of unconfined charges exceeding 250 mm diameter and 1500 mm length.

The measurements for COMP B have sampled across the full range of extents of reaction, but only for a restricted part of the pressure domain. Consequently, descriptions of low pressure shock initiation based only on the CPeX fit would be suspect unless augmented by specific initiation experiments. However, the reaction rate surface for HANFO is very well covered by the experimental detonation velocity data, permitting accurate predictions of its detonics.

CJ PRESSURE

Figure 4 presents the CPeX predictions for the pressures at the shock front, and at the CJ plane. It can be seen that they are predicted to vary by a factor of about three over the full range of diameters that will support detonation.

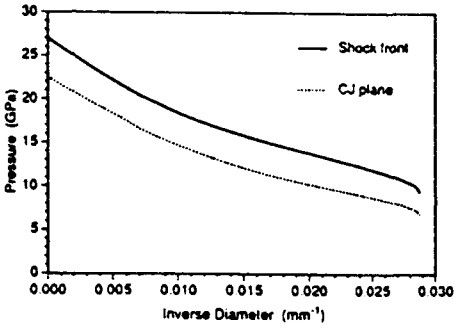

FIGURE 4. CPeX SHOCK AND CJ PRESSURES

HYDROCODE MODELLING OF PBXW-115

The equation of state and reaction rate law described above for the CPeX model were embedded in the explicit finite element hydrocode DYNA2D[5] to permit the simulation of time-dependent reactive flow in non-ideal explosives. The constants derived for PBXW-115 by the CPeX analysis, and displayed in Table 3, were used in the DYNA2D simulations without any further adjustment.

STEADY-STATE AXISYMMETRIC DETONATION

Figure 5 summarises the DYNA2D predictions of detonation velocity in axisymmetric geometry. All charges were 300 mm in length to ensure that steady state conditions were reached. There is excellent agreement between the numerical simulations and the experimental data[1] for both unconfined and confined detonations in 2.5 mm thick brass.

The experimental[1] pass / fail diameters for PBXW-115 were 38.7 / 35.1 mm unconfined, and 22.2 / 19 mm confined (in 2.5 mm brass). The simulations were in excellent agreement, predicting 38 / 37 mm unconfined and 22 / 19 mm

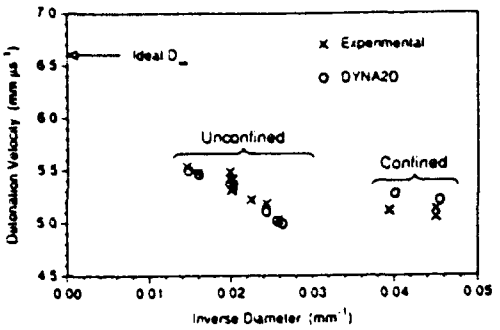

FIGURE 5. PBXW-115 DETONATION VELOCITY

confined. Figure 6 shows how the predicted shock velocity in a 37 mm rate stick decayed with distance from the booster. The wave propagated for over four charge diameters before dying. Dick[16] has observed similar behaviour for a HMX-based composite propellant. This suggests that the 153 mm length charges used at NSWC were only just long enough to ensure steady state behaviour in diameters close to critical.

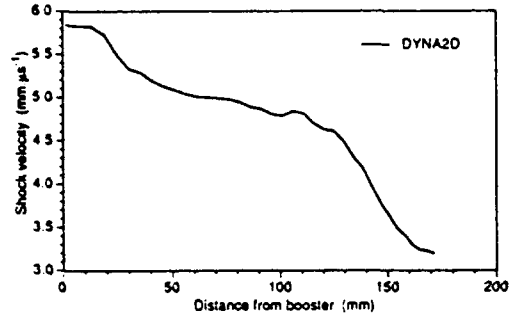

FIGURE 6. FAILURE IN 37MM DIAMETER

This high level of agreement for unconfined detonation confirms not only the model constants, but also serves to verify the assumptions made in the CPeX model to relate flow divergence to shock front curvature. Such assumptions are not required for the DYNA2D simulations. Furthermore, the similar excellent agreement for confined detonation provides additional confirmation of the model, having sampled a different combination of lateral expansion and extent of reaction.

WAVE FRONT CURVATURE AND CJ ZONE LENGTHS

Figure 7 presents the comparison between the NSWC measurements[1] and the DYNA2D simulations of shock front radius of curvature for unconfined charges, plotted to illustrate the linear behaviour expressed in equation (18). The scatter reflects the difficulty in measuring the curvature both experimentally and in the simulations. This data was used in the CPeX fit, but not explicitly by the DYNA2D simulations. The good agreement thus helps to confirm the flow pattern assumed in the CPeX theory.

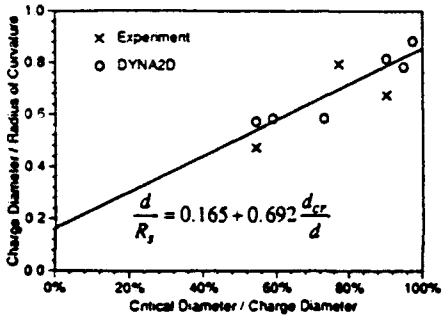

FIGURE 7 SHOCK FRONT CURVATURE

Wave curvature experiments are often performed in order to estimate the CJ zone lengths via application of the Wood-Kirkwood theory.[10] The zone lengths calculated by Forbes et al.[1] are compared with the CPeX predictions in Figure 8. The agreement is poor, with the CPeX CJ zone lengths being up to a factor of two higher than Forbes' calculations based on

$$\frac{D_\infty - D}{D_\infty} = C\frac{x_{CJ}}{R_s} \qquad (19)$$

where D_∞ is the ideal value of the detonation velocity, D the measured value, and R_s the wave curvature for the charge diameter of interest. C is a constant dependent upon the equation of state. Wood and Kirkwood derived equation (19) as a specific solution to their more general theory by making a number of assumptions. In particular, they assumed that the reaction rate is Arrhenius in form, so that the reaction rate immediately behind the shock is low, and then rises to a sharp maximum very close to complete reaction. This leads firstly to CJ parameters (ρ, v and λ), that are only slightly perturbed from their ideal values, and secondly to a pressure profile that is essentially flat-topped at the von Neumann spike value. These conditions are not too dissimilar from the behaviour summarised in Figures 2 and 3 for the ideal explosive COMP B. However, these Figures show that these assumptions are clearly inappropriate for both non-ideal explosives, PBXW-115 and HANFO. Hence, the simplistic form of the Wood-Kirkwood theory, represented by equation (19), should not be applied to non-ideal explosives.

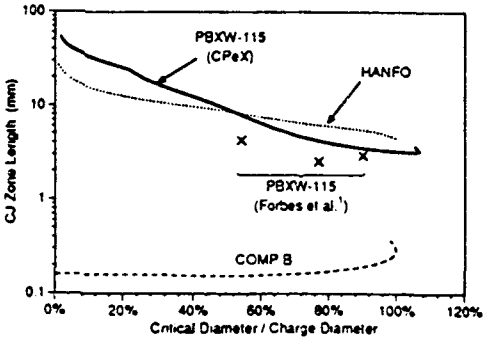

FIGURE 8. CPeX CJ ZONE LENGTHS

It is apparent from Figure 8 that the CJ zones for the two non-ideal explosives extend over much larger regions of space than is the case for the ideal one. In particular, it is predicted that experiments intended to characterise an ideal steady-state planar detonation in PBXW-115 must be performed on a massive scale — the ideal CJ zone predicted by CPeX exceeds 60 mm in length and 15 μs in duration.

CORNER TURNING

Forbes et al.[1,2] have characterised the corner-turning ability of PBXW-115, measuring the breakout times through

the curved surfaces of bowl-shaped acceptor charges. The bowls were initiated through their flat rear surfaces by boosters of 51 mm diameter and 153 mm in length. The curved surface of each bowl had a radius of curvature of 51 mm (measured from the edge of the booster). Four different booster configurations were used — (1) bare PBXW-115, (2) bare COMP B, (3) bare COMP B with a steel plate covering the flat surface of the bowl, and (4) PBXW-115 confined in a brass tube with 16.5 mm thick walls.

In order to control the distortion of the finite element mesh at the booster/bowl junction, it was necessary to introduce a 6 mm radius of curvature there in the numerical simulations with DYNA2D — the effect of this change on the predicted breakout times is unknown, but is believed to be small. Figure 9a presents the predicted pressure contours 9 μs after the shock from the booster has entered the bowl, while Figure 9b shows the extent of reaction after the shock has completely enveloped the bowl (with the material motion removed in order to facilitate comparison).

The comparison with experiment is shown in Figure 10, and is seen to be excellent for the bare boosters, cases (1), (2), and (3). This agreement indicates that the reaction rate surface for PBXW-115 (shown in Figure 3a) is accurate in regions beyond that directly calibrated by the detonation velocity measurements. In particular, the breakout through the outer edges of the bowl for case (1), the unconfined PBXW-115 booster, is controlled by the reaction rate surface in the lower pressure regime below about 5 GPa. The breakouts for cases (2) and (3) with the COMP B boosters are dominated by the high pressures, exceeding 20 GPa, developed along the axis of the bowls.

The lack of agreement for case (4), the confined PBXW-115 booster, was unexpected. Both the experimental detonation velocity data and the associated simulations summarised in Figure 5 prove that even thin (2.5 mm) brass confinement makes a significant difference to detonation in PBXW-115, decreasing the critical diameter by a factor of roughly two. The confinement in the corner turning experiment was a brass tube with thick (16.5 mm) walls, and hence should increase both the peak value and the duration of the pressure delivered

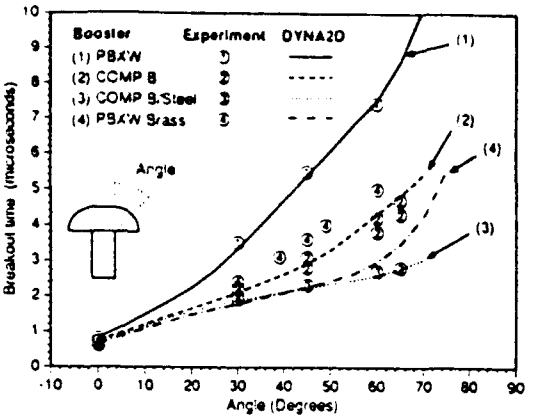

FIGURE 10. CORNER TURNING BREAKOUT TIMES

by the booster to the acceptor charge. Furthermore, the shock wave in the brass confinement enters the bowl in concert with that from the booster, increasing the area over which pressure is applied to the bowl. These factors should all combine to appreciably shorten the breakout times through the outer edges of the bowl. No plausible explanation for the discrepancy between experiment and simulation could be found.

WEDGE TEST AND POP-PLOTS

The wedge test is often used to characterise the shock initiation behaviour of explosives. A plane-wave generator sends a relatively flat-topped planar shock into a wedge of acceptor explosive — observation of the emergence of the shock through the angled face of the wedge gives a continuous record of run up to detonation. The results are displayed on a Pop-plot, where the measured run distance to detonation is plotted against the initial shock pressure.

Although PBXW-115 has not been investigated experimentally by this technique, several simulations were performed to predict its likely behaviour. Figure 11 summarises the predicted shock velocity-time trajectories over a 50 mm run distance induced by various input shock

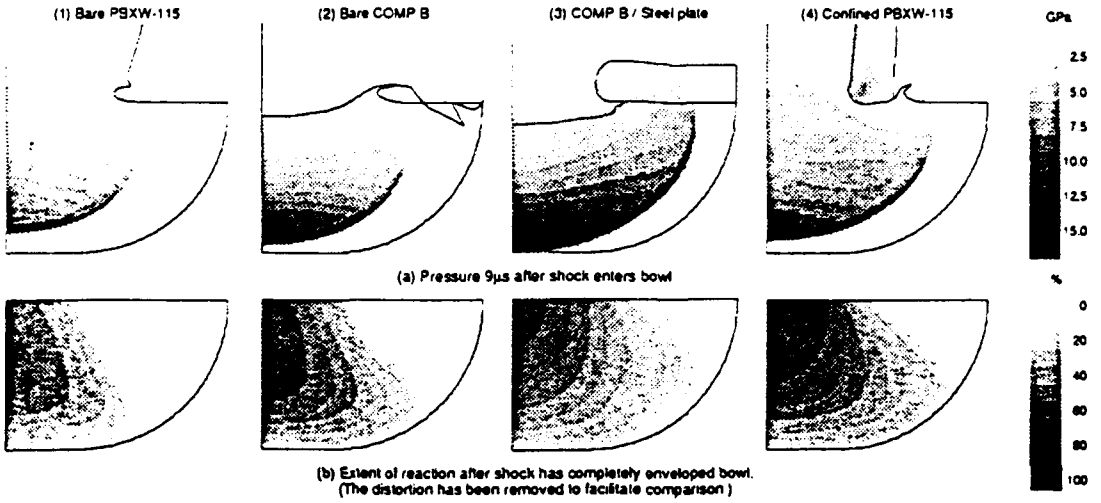

FIGURE 9. EFFECT OF BOOSTER TYPE ON CORNER TURNING IN BOWL OF PBXW-115.

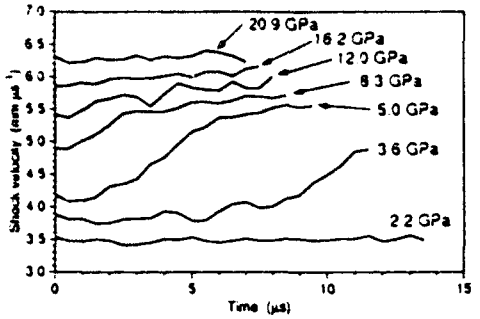

FIGURE 11. PREDICTED SHOCK ACCELERATION OVER 50 MM IN WEDGE TEST

pressures. In the simulations, these pressures were created by the impact of thick aluminium flyer plates.

These trajectories are notable for the absence of the sharp transition between low velocity shock and high velocity detonation that is characteristically observed with ideal explosives. They are qualitatively similar to those published for other non-ideal explosives. Dick[16] suggested that the gradual increase of velocity with time shown by the traces for a HMX / AP / Al / binder propellant (not unlike PBXW-115) was evidence of overdriven detonation. In spite of all trajectories showing gradual acceleration, workers at RCEM[17,18] derived a Pop-plot for an emulsion explosive, concluding that it was much less shock sensitive than TNT.

The present work suggests that these interpretations of wedge test data for non-ideal explosives are incorrect. Figure 12 extends the trajectories of Figure 11 out to a distance of 500 mm. Two features are apparent. Firstly, the trajectories for the 2.2 and 3.6 GPa initial shocks now show clear transitions between low and high velocity regimes. Secondly, none of the trajectories have attained a steady-state velocity even after 500 mm of run, though they are all asymptoting towards the expected ideal detonation velocity of 6.67 mm.μs^{-1}.

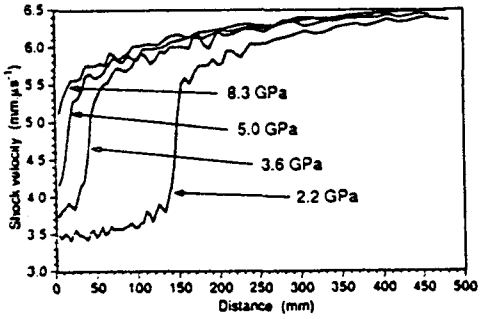

FIGURE 12. PREDICTED SHOCK ACCELERATION OVER 500 MM IN WEDGE TEST

This behaviour can be explained by referring to the reaction rate surfaces in Figure 3. For PBXW-115, the λ surface can be divided into two regimes.

Firstly, for initial shock pressures above 5 GPa, the peak reaction rate occurs at minimal extents of reaction, causing rapid consumption of the RDX component. Any rapid acceleration of the shock velocity will occur during this short phase, quickly giving rise to velocities typical of detonation in small diameters, ie. about 5.0 - 5.5 mm μs^{-1}. However, once the extent of reaction exceeds 20% or so, the reaction rate decreases sharply, and so approach to the ideal detonation state will be gradual.

Secondly, for initial shock pressures below 5 GPa, the initial reaction rate is low, so that the shock propagates with minimal acceleration. However, as the reaction proceeds and the pressure builds up, the condition is reached where the reaction rate increases sharply. The shock then makes a sharp transition to a higher velocity, though, as above, it is supported essentially by consumption of the RDX. Further acceleration is consequently slow.

In contrast, ideal explosives at low porosity will have reaction rate surfaces similar to that shown in Figure 3c for COMP B. Here, the initial reaction rate at low to medium shock pressures is low, so that initial shock velocities are low with minimal acceleration. However, once several percent reaction has occurred, the increase of pressure causes the rapid acceleration of the reaction rate, resulting in an abrupt transition. Furthermore, the reaction rate remains high, so that the reaction soon goes to completion, and the ideal detonation velocity is quickly attained. Hence, there is always a strong distinction between detonation and non-detonation.

This analysis suggests that reduction of wedge test traces, and interpretation of their resultant Pop-plots, requires substantial modification for non-ideal explosives. Pop-plots are traditionally used for two distinct purposes. Firstly, they are used to derive kinetics for detonation models, as exemplified by the Forest-Fire model[19]. However, this paper has shown how this can be accomplished instead by detonation velocity measurements on non-ideal explosives. Secondly, they are used to rank the shock sensitivity of different explosives for hazard studies. For this purpose, it is sufficient to know the conditions under which incident shocks lead to self-propagating reactive waves releasing substantial amounts of energy. Hence, it is necessary to replace the identification of transition to detonation by the identification of transition between low and high velocity shocks.

Once this is done, Figures 11 and 12 show that PBXW-115 exhibits such transitions for incident shock pressures below 5.0 GPa. The resulting Pop-plot is shown in Figure 13, where it can be seen that PBXW-115 exhibits a greater hazard to low strength shocks than either TNT or Baratol, both of which have much smaller critical diameters.

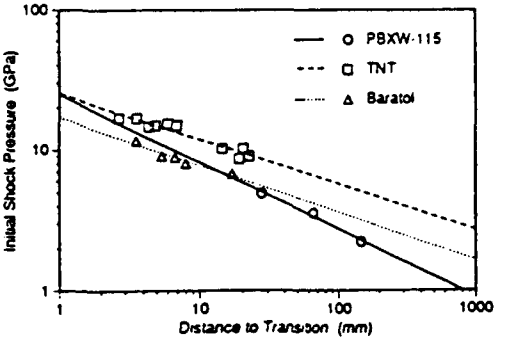

FIGURE 13. PREDICTED POP-PLOT FOR PBXW-115

The wedge test behaviour of other non-ideal explosives can now be explained.

In the propellant studied by Dick[16], HMX would play the role of the RDX in PBXW-115 — Figure 1 of Dick's paper does indeed show a strong similarity to Figure 11 of this work, though shifted to higher initial shock pressures in line with the lower inherent shock sensitivity of HMX when compared with RDX.

The emulsion studied at RCEM[17,18] is expected to have a reaction rate surface not unlike that of the HANFO shown in Figure 3b. This exhibits only the first regime discussed above, where the reaction rate is always greatest at or immediately behind the shock front, so that acceleration is always smooth, and transitions would never occur. Hence, both the published Pop-plot for this emulsion, and the claim that it is less sensitive than TNT, are suspect.

IDEAL DETONATION VELOCITY EXPERIMENT

Held[4] has recently described a technique to measure the ideal detonation velocity using only small samples, and has applied it to the German variant of PBXW-115. A donor charge with high detonation velocity drives a bow wave into a parallel adjacent acceptor test charge with lower detonation velocity, which is inferred from the measurement of the breakout through the face opposite the initiation point. Held assumed that if a steady detonation was established in the acceptor, then it must represent an ideal detonation.

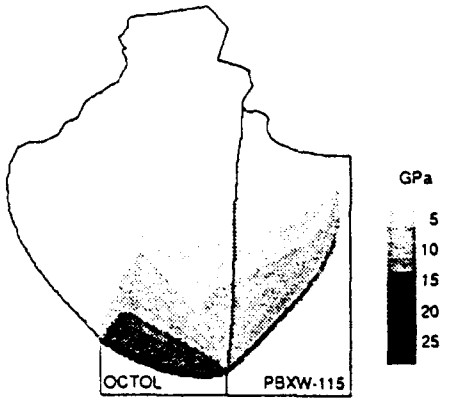

(a) Pressure

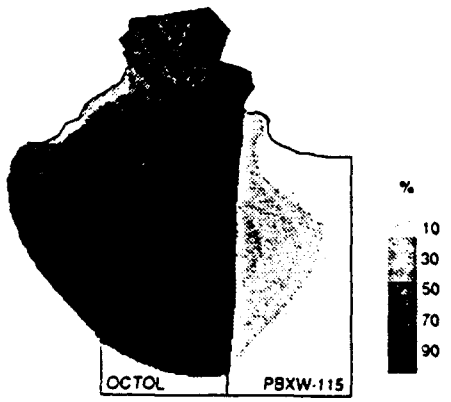

(b) Extent of Reaction

FIGURE 14. DYNA2D PROFILES FOR IDEAL DETONATION VELOCITY METHOD

Figure 14 shows the predicted detonation wave shapes immediately prior to breakout for the case of an Octol donor driving a bow wave into PBXW-115. Although the bow wave in the PBXW-115 is shown as being curved, DYNA2D predicts that it does become straight prior to full breakout. (This simulation had to be performed using slab charges in planar geometry, in place of the actual half cylinders. The PBXW-115 used in the experiments had the composition 40 / 24 / 24 / 12% AP / RDX / Al / binder. This was treated by increasing Φ_h to 18% and decreasing Φ_i to 57%.)

The charges used by Held were 60 mm in length, which is roughly the same order as the ideal CJ zone length predicted by CPeX (shown in Figure 8). Consequently, DYNA2D is predicting that a steady non-ideal detonation has been created in the PBXW-115, with the extent of reaction having reached a maximum of less than by 50% by the time that the detonation front begins to break out through the end face.

The predicted breakout times for the non-ideal detonation are compared with the experimental results in Figure 15, with the agreement being excellent, confirming the accuracy of the DYNA2D simulation. The conclusion is that the small sample technique does not measure ideal detonation velocity as intended. Much longer and larger diameter charges would be required to accomplish this objective.

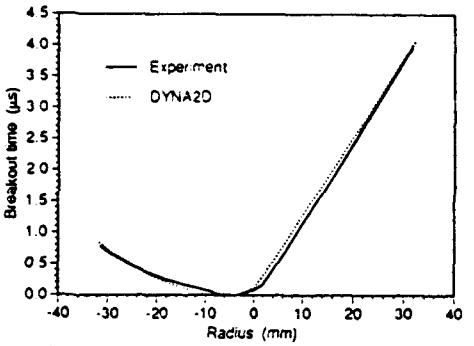

FIGURE 15. BREAKOUT TIMES FOR IDEAL DETONATION VELOCITY METHOD

CONCLUDING REMARKS

The application of the CPeX small-divergent detonation theory, and the DYNA2D simulations performed for this paper, have both been built around the assumption that the ideal detonation velocity of PBXW-115 is 6.67 mm.μs^{-1} as predicted by the chemical equilibrium code IDeX.[7] At the time of writing, there is no direct experimental evidence to support this assumption. However, the ensuing excellent agreement between the predictions and almost all the available experimental data provides strong indirect evidence that this assumption is correct, and hence that the detonics of PBXW-115 are strongly non-ideal.

The only piece of experimental data which could not be reproduced by the DYNA2D simulations was the breakout time in one configuration of the corner turning experiments. Strangely, the simulations did successfully reproduce the breakout times of the two configurations that were found experimentally to bracket the offending configuration.

The analysis presented in this paper illustrates that the

reaction rate surface of the non-ideal explosive PBXW-115 is fundamentally different from that of the ideal explosive, Composition B. It is strongly believed that this is a specific example of a more general truth.

Many of the experimental tests in use today were developed to characterise the detonics of ideal explosives, and at a fundamental level, require the reaction rate surface to have particular features. When applying such tests to non-ideal compositions, it is essential to understand the basis of what the test is actually measuring in order to know if it is still applicable. In particular, if knowledge of the full range of detonation behaviour is required for an explosive like PBXW-115, there is no way to avoid at least some experiments performed on massive charges.

Many of the theories and the data reduction techniques that are applied to detonation experiments assume that non-ideal behaviour can be treated as a small perturbation in (p, v, λ) space from the ideal CJ conditions. However, a steady-state detonation that is supported by only about 15% reaction cannot be considered to represent a small perturbation from ideal. Due to the work by Forbes and co-workers at NSWC,[1,2] there is now an extensive database of experimental information available on at least one non-ideal explosive for use in confirming the miriad emerging theories of non-ideal detonics.

ACKNOWLEDGMENTS

A number of people have provided invaluable advice, information, and discussion during this work. Through the TTCP agreement, Jerry Forbes made available his comprehensive experimental data prior to publication. Dan Whelan and Gunter Bocksteiner provided information and insights on the behaviour of the Australian variant of PBXW-115. Chuck Mader advised on the application of BKW to non-ideal systems. Bob Sheahan and Gwyn Harries provided many insights into non-ideal detonics. Graeme Leiper contributed much advice on the application of CPeX to PBXW-115, while Alan Minchinton explained many of the finer details of the CPeX model.

The authors acknowledge with thanks the permission of ICI Australia and of DSTO to publish this paper.

REFERENCES

1. Forbes, J. W.; Lemar, E. R.; and Baker, R. N., "Detonation Wave Propagation in PBXW-115", *Ninth Symposium (International) on Detonation*, Office of the Chief of Naval Research, OCNR 113291-7, 1989, pp.806-815.

2. Forbes, J. W.; Lemar, R.; and Baker R., "Detonation wave corner turning in PBXW-115", Bulletin of American Physical Society, Vol 35, No. 3, March 1990, p.808.

3. Bocksteiner, G.; and Wolfson, M., *Detonation velocity measurements on Australian PBXW '15*, Materials Research Laboratory report, Melbourne, in press 1993.

4. Held, M., "Steady Detonation Velocity D_∞ of Infinite Radius Derived from Small Samples", *Propellants, Explosives and Pyrotechnics*, Vol 17, 1992, pp. 275-277.

5. Hallquist, J. O., *User's Manual for DYNA2D*, UCID-18756, Rev 3, March 1988, Lawrence Livermore National Laboratory, Livermore, CA.

6. Mader, C. L., *FORTRAN BKW A code for computing the detonation properties of explosives*, LA-3704, Los Alamos Scientific Laboratory.

7. Freeman, T. L.; Gladwell, I.; Braithwaite, M.; Byers-Brown, W.; Lynch, P. L.; and Parker, I. B., "Modular software for modelling the ideal detonation of explosives", *Math. Engng. Ind.*, Vol 3, No 2, 1990, pp.97-109.

8. Jeanloz, R., "Shock Wave Equation of State and Finite Strain Theory", *Journal of Geophysical Research*, Vol 94, No B5, 1989, pp. 5873-5886.

9. Kirby, I. J.; and Leiper, G. A., "A small divergent detonation theory for intermolecular explosives", *Proceedings of the Eighth Symposium (International) on Detonation*, Albuquerque, 1985, pp. 176-185.

10. Wood, W. W.; and Kirkwood, J. G., "Diameter effect in condensed explosives. The relationship between velocity and radius of curvature of the detonation wave", *Journal of Chemical Physics*, Vol 22, 1954, pp. 1920-1924.

11. Braithwaite, M.; Farran, T.; Gladwell, I.; Lynch, P. M.; Minchinton, A.; Parker, I. B.; and Thomas, R. M., "A detonation problem posed as a differential/algebraic boundary value problem", *Math. Engng. Ind.*, Vol 3, No. 1, 1990, pp. 45-57.

12. Leiper, G. A., private communication to D. L. Kennedy regarding literature survey of wave curvature, 1988.

13. Malin, M. E.; Campbell, A. W.; and Mautz, C. W., "Particle-Size Effects in Explosives at Finite and Infinite Diameters", *Journal of Applied Physics*, Vol 28, No. 1, 1957, pp. 63-69.

14. Afanasenkov, A. N.; Bogolomov, V. M.; and Vostobionikiv, I. M., "Generalised shock Hugoniot of condensed substances", *Zhur. Prok. Mekh. Tekh.*, Vol 10, 1969, pp. 137-147.

15. Gibbs, T. R.; and Popolato, A.; Eds., *LASL Explosive Property Data*, University of California Press, Berkeley, 1980, p. 416.

16. Dick, J. J., "Nonideal detonation and initiation behaviour of a composite solid rocket propellant", *Seventh Symposium (International) on Detonation*, Naval Surface Weapons Center, NSWC MP 82-334, 1982, pp. 620-623.

17. Sandstrom, F. W., *Shock initiation characteristics of composite energetic materials*, Research Center for Energetic Materials, New Mexico, RCEM Semiannual Technical Report A-03-89, 1989, pp. 22-25.

18. Lee, J.; Sandstrom, F. W.; Craig, B. G.; and Persson, P. A., "Detonation and shock initiation properties of emulsion explosives", *Ninth Symposium (International) on Detonation*, Office of the Chief of Naval Research, OCNR 113291-7, 1989, pp.573-584.

19. Mader, C. L., *Numerical Modelling of Detonation*, University of California Press, Berkeley, 1979, pp. 208-250.